Best-Fit Techniques to Estimate SBU/MCU Cross Sections from Radiation-Ground Tests in Memories

Francisco J. Franco, Juan C. Fabero, Hortensia Mecha, Mohammadreza Rezaei, Guillaume Hubert, and Juan A. Clemente

Abstract

This paper studies the probability distribution for the expected number of bitflips per round of reading in radiation-ground tests on a memory device where only single bit upsets and multiple cell upsets occur. This distribution is used to estimate the soft error cross sections in actual experiments by means of two best-fit approaches, one based on the gradient descent algorithm, the other on genetic algorithms. Besides, it is investigated how this mathematical study is suitable to detect possible variations in the soft error rate due to different reasons, such as variations in the radiation flux. Finally, the inherent stochastic characteristics of the experiments are used to provide tools to detect forgery in experiment data.

Index Terms

SBU, MCU, SRAM, Radiation-ground test.

I. Introduction

In a radiation-ground test performed on memories, it is essential to make a correct interpretation of the events that were observed after each round of reading, in order to discern between Single Bit Upsets (SBUs) and Multiple Cell Upsets (MCUs) from the whole set of bitflips. This is easy to do if the internal organization of the device is known. However, this knowledge is seldom available to researchers as it is intellectual property from manufacturers. Hence, several researches have proposed alternative techniques to estimate the amount of MCUs occurred using statistical properties of the radiation data sets.

Some techniques in the literature consist in extracting the mapping relation between the least significant bits of the device's physical address and the logical address bits [1], [2] in order to guess its interleaving architecture. Another approach consists in detecting statistical anomalies in the datasets by combining all addresses affected by bitflips in the same round of reading by using a binary operator (such as subtraction or bitwise XOR), and then identifying the values that are repeated more often than expected with respect to a theoretical scenario where no MCUs occur [3]–[9].

In [10], Pérez-Celis et al. pointed out an interesting fact: some statistical properties can also be observed in the number of bitflips per round of reading in radiation-ground tests consisting in a sufficiently high amount of such rounds (i.e., tens or hundreds) under identical conditions during all the test. In this situation, they were able to distinguish and discard those rounds where Single Event Functional Interrupts (SEFIs) had occurred, thus making a more accurate analysis to extract MCUs from the set of observed bitflips.

However, even though the simple Poisson distribution proposed in [10] was useful to just detect SEFIs in some rounds of reading, the actual statistical distribution modeling the probability of occurrence of bitflips per round of reading is more sophisticated, and it is necessary to estimate the number of events with different multiplicities (SBUs/MCUs) that were observed in the radiation-ground experiment. The objective of this paper is to provide an accurate estimation of that probability distribution. Thus, the next section of this paper will present a finer model of this distribution and its properties. Next, two best-fit techniques to estimate the number of SBUs/MCUs observed in a radiation-ground test will be presented and finally, these techniques will be validated with experimental data and compared with another statistical technique, also presented by the authors in previous works [6]–[8]. Finally, the theoretical statistical properties of these experiments are proposed as tools to determine if the radiation tests are correctly done and interpreted.

II. Statistical Properties of Pseudo-Static Tests

Let us suppose that a memory device was irradiated in N_R rounds of reading, all of them identical in terms of particle fluence and environmental conditions, and received ϕ particles/cm^2 per round. Therefore, the total fluence is

$$\Phi_T = N_R \cdot \phi.$$

This work was supported by the Spanish MICIINN project PID2020-112916GB-I00.

F. J. Franco is with the Department of Structure of Matter, Thermal Physics, and Electronics, Facultad de Ciencias Físicas, Universidad Complutense de Madrid (UCM), 28040 Madrid, Spain, e-mail: fjfranco@fis.ucm.es.

J. C. Fabero, H. Mecha, M. Rezaei and J. A. Clemente are with the Computer Architecture Department, Facultad de Informática, Universidad Complutense de Madrid (UCM), 28040 Madrid, Spain, e-mail: { jcfabero, horten, mrezaei, juanancl}@ucm.es.

G. Hubert is with the ONERA French Aerospace Laboratory, 31000 Toulouse, France, email: guillaume.hubert@onera.fr

At the end of the experiment and after identifying and removing flipped cells attributed to stuck bits (repeated addresses in different rounds) along with those large error clusters related to SEFIs [10], leaving only SBUs and MCUs, N_T bitflips were registered in the devices, of which only events up to m-multiplicity are expected to occur, and larger events are negligible. Hence, let $N_{E,i}$ be the total number of events of i-multiplicity. Every possible event with i-multiplicity has its own cross section value *per device*, σ_i, with $i \in [1, 2, \ldots, m]$. It follows that the expected number of events of i-multiplicity in each round is

$$\mu_i = \phi \cdot \sigma_i. \tag{1}$$

As the cross section depends on several parameters, it is mandatory to keep their values constant during the irradiation: ion species and energy; incidence angle or, in other experiments, isotropic flux; written pattern, which must not change from round to round. Also, it is advisable to keep the received fluence per round low enough to avoid the occurrence of false multiple events if other strategies to calculate cross sections of multiple events will be used with the same data set [11]. Besides, it is well known that the probability of occurrence of k events of i-multiplicity in a round follows a Poisson distribution defined as

$$P_i(k) = e^{-\mu_i} \cdot \frac{\mu_i^k}{k!}, \quad i \in 1, 2, \ldots, m;\ k \in \mathbb{N} \cup \{0\}. \tag{2}$$

After each round, researchers can only see a set of bitflips originating in an unknown number of events of different multiplicities, each one with its particular expected number of occurrences per round, μ_i. The objective of the techniques presented in this paper is to estimate these values. i For this purpose, let us define the *decomposition* of a natural number n on a set $(1, 2, \ldots, m)$ as the m-tuple of natural numbers $(a_1, a_2, \ldots, a_m)$ such that

$$n = \sum_{i=1}^{m} a_i \cdot i. \tag{3}$$

In other words, a decomposition is just a solution for a linear Diophantine equation with several unknowns. There can be several possible decompositions of a given number n. For example, there exist 7 possible decompositions of $n = 6$ and $m = 3$, namely:

- $6 \cdot \mathbf{1} + 0 \cdot \mathbf{2} + 0 \cdot \mathbf{3}$
- $4 \cdot \mathbf{1} + 1 \cdot \mathbf{2} + 0 \cdot \mathbf{3}$
- $3 \cdot \mathbf{1} + 0 \cdot \mathbf{2} + 1 \cdot \mathbf{3}$
- $2 \cdot \mathbf{1} + 2 \cdot \mathbf{2} + 0 \cdot \mathbf{3}$
- $1 \cdot \mathbf{1} + 1 \cdot \mathbf{2} + 1 \cdot \mathbf{3}$
- $0 \cdot \mathbf{1} + 3 \cdot \mathbf{2} + 0 \cdot \mathbf{3}$
- $0 \cdot \mathbf{1} + 0 \cdot \mathbf{2} + 2 \cdot \mathbf{3}$.

Coming back to our problem, a decomposition of a number of bitflips n can be seen as a conjecture about the expected number of events of different multiplicities (ranging from 1 to m) that were observed in a round of reading. Hence, the example above is equivalent to the fact that, if 6 bitflips were observed in a round, they could have originated either in six SBUs; or in four SBUs and two 2-bit MCUs; or in three SBUs and one 3-bit MCU, etc. However, each one of these decompositions has its own probability of occurrence, which can be estimated as follows. In a round where n bitflips were observed, let $A_{m,n}$ be the set of possible decompositions of n on the set $\{1, 2, \ldots, m\}$. Thus, every decomposition $d_j \in A_{m,n}$ is described with an m-uple of natural numbers, $a_1, a_2, \ldots, a_m$. Going on with the previous example, if $n = 6$ and $m = 3$, the seven possible decompositions, $d_j = (a_1, a_2, a_3)$, are:

- $d_1 = (6, 0, 0)$
- $d_2 = (4, 1, 0)$
- $d_3 = (3, 0, 1)$
- $d_4 = (2, 2, 0)$
- $d_5 = (1, 1, 1)$
- $d_6 = (0, 3, 0)$
- $d_7 = (0, 0, 2)$.

The probability $P(d_j)$ of having observed n bitflips and that the decomposition of n into multiple events being precisely $d_j \in A_{m,n}$ is just the product of the probabilities of a_1, a_2, ..., a_m events with different multiplicities occurring in that decomposition. For instance, the probability of occurrence of $d_j = (a_1, a_2, a_3)$ is the product of the probabilities of a_1 SBUs, a_2 2-bit MCUs and a_3 3-bit MCUs occurring simultaneously, each one of them being calculated with a Poisson distribution with μ_1, μ_2 and μ_3, respectively. As the probability of every type of event is modeled by Eq. (2), and $P(d_j)$ is the product of all of them, it can be estimated as

$$\begin{aligned} P(d_j) = \\ = e^{-\mu_1} \cdot \frac{\mu_1^{a_1}}{a_1!} \times e^{-\mu_2} \cdot \frac{\mu_2^{a_2}}{a_2!} \times \ldots \times e^{-\mu_m} \cdot \frac{\mu_m^{a_m}}{a_m!} = \\ = \exp\left(-\sum_{i=1}^{m} \mu_i\right) \cdot \prod_{i=1}^{m} \frac{\mu_i^{a_i}}{a_i!}. \end{aligned} \tag{4}$$

However, several decompositions can lead to the same number of observed bitflips, n. Thus, the probability of having observed n bitflips in a round of reading, under any decomposition among the possible ones, is the sum of the probabilities of all the values of $P(d_j)$ within $A_{m,n}$. This yields the following global probability distribution:

$$P_G(n) = \exp\left(-\sum_{i=1}^{m}\mu_i\right) \cdot \sum_{d_j \in A_{m,n}} \left(\prod_{i=1}^{m} \frac{\mu_i^{a_i}}{a_i!}\right). \tag{5}$$

Values of $P_G(n)$ for $n = 0$ and $n = 1$ can be easily calculated, since they only admit the decompositions $(0, 0, \ldots, 0)$ and $(1, 0, \ldots, 0)$, thus yielding

$$P_G(0) = \exp\left(-\sum_{i=1}^{m}\mu_i\right), \tag{6}$$

and

$$P_G(1) = \exp\left(-\sum_{i=1}^{m}\mu_i\right) \cdot \mu_1. \tag{7}$$

It follows that the expected number of rounds where n bitflips were detected is

$$N_r(n) = N_R \cdot P_G(n). \tag{8}$$

Eqs. (4) and (5) are implicit probability distributions that must be numerically computed beyond the trivial case of $m = 1$ (which becomes the Poisson distribution since only one decomposition is possible in that case). Fig. 1a shows the expected shapes of the distribution (Probability Mass Function or PMF) of Eq. (4), for $n = 10$ and $m = 3$, whereas Fig. 1b shows their Cumulative Mass Functions (CMF). As we can see, those distributions with $\mu_1 = 6, \mu_2 = 2$, and $\mu_1 = 3, \mu_2 = 2, \mu_3 = 1$ have a similar shape as the Poisson distribution for $\mu_1 = 10$, although broader and with a lower central peak.

Numerical calculations allow postulating that the mean value, μ_T, and the variance, (σ_T^2), of the implicit distribution of Eq. (5) are

$$\mu_T = \sum_{i=1}^{m} i \cdot \mu_i, \tag{9}$$

and

$$\sigma_T^2 = \sum_{i=1}^{m} i^2 \cdot \mu_i. \tag{10}$$

These facts are extremely difficult to infer from Eq. (5) by applying the formal definitions due to its complexity and absence of closed forms. However, both expressions are easily derived from some simple properties of statistical distributions. The key point is that the ocurrence of bitflips in a single round is just the overlay of different phenomena (SBUs, 2-bit MCUs, etc.), which are statistically independent[1]. Therefore, the expected amount of bitflips per round associated with SBUs is μ_1, with 2-bit MCUs $2 \cdot \mu_2$, etc. The theory of probability provides some universal results for independent statistical variables regardless of their own probability distribution. First of all, the average value of a linear combination of variables is the linear combination of average values (See Theorem 6.1 in [12]). Hence, Eq. (9) immediately follows.

There are other two universal results for independent variable. First of all, if a variable is multiplied by α, a real number, to become a new statistical variable, the variance of this new variable is

$$\alpha^2 \cdot \sigma^2,$$

σ^2 being the variance of the initial variable (Th. 6.7 in [12]). Also, the variance of the sum of variables is the sum of variances (Th. 6.8 in [12]). Combining these properties of independent statistical distributions with that of the Poisson distribution immediately leads to Eq. (10).

In short, Eq. (5) makes possible to explicitly write the probability distribution of $P_G(n)$ in terms of values μ_i, which are the expected number of events with i-multiplicity. These values are initially unknown at this point of the discussion. The objective of the techniques proposed in Section III is to provide an accurate estimation for these values.

Finally, be aware of not misleading the cross sections (σ_i) and the variance (σ_T^2), as both parameters are symbolized by the same Greek letter.

[1]This independence disappears if some cells are flipped twice or more, but this fact is usually negligible.

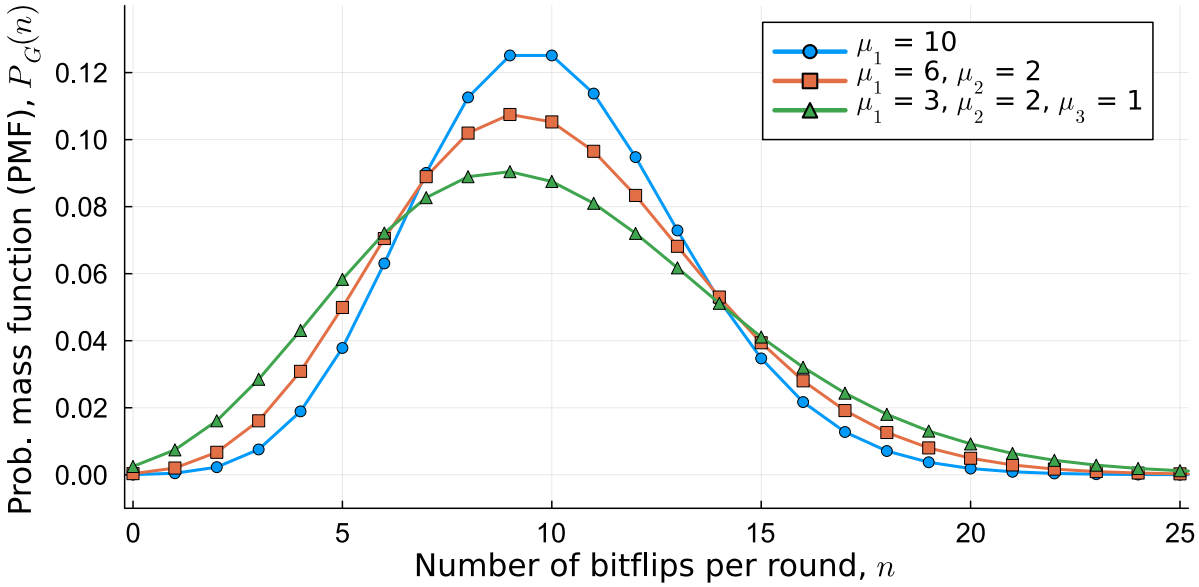

(a)

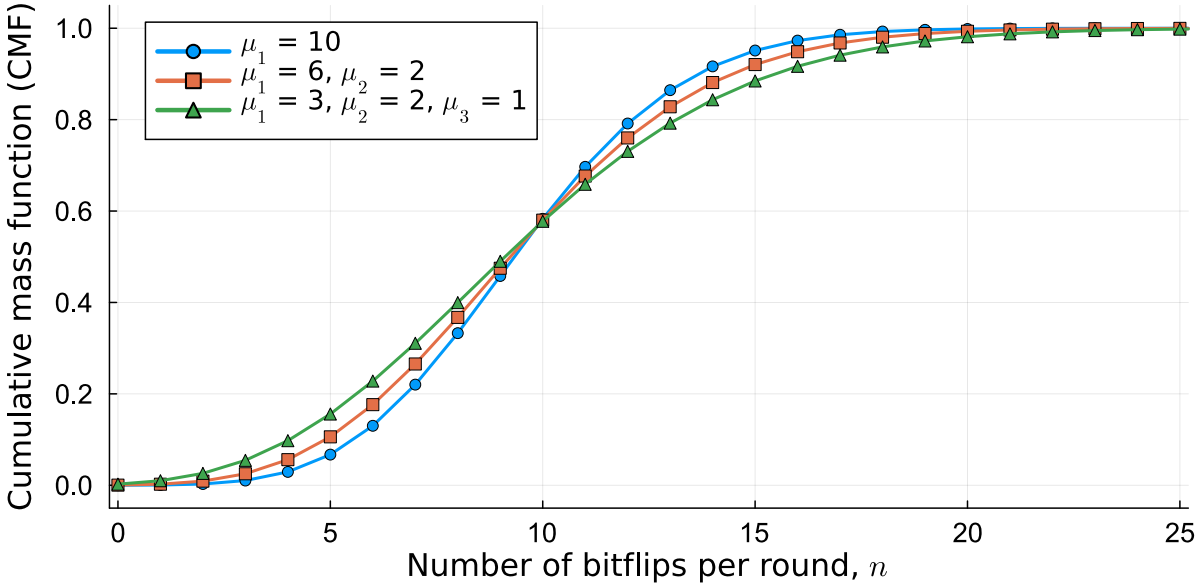

(b)

Fig. 1. Probability mass functions (a) and cumulative mass functions (b) of the number of expected bitflips per round of reading, assuming three possible decompositions of $n = 10$. The former is obtained from Eq. (5), whereas the latter is defined as the partial sum of values of $P_G(n)$ lower than or equal to n. For each case, the number of expected events are indicated in the legends.

III. Techniques Proposed to Estimate SBU/MCU Cross Sections

This section presents two best-fit techniques to estimate the values of $\mu_1, \mu_2, \ldots, \mu_m$, discussed in Section II.

Firstly, let us assume a radiation-ground test on a memory consisting in N_R identical rounds of reading. In general terms, N_n is the number of rounds where n bitflips were actually observed in the radiation-ground test: N_0 rounds yielded no bitflips, N_1 did only one, N_2 two, etc. Hence, one can build up the set of ordered pairs, (n, N_n), with $0 \leq n \leq T$, T being the maximum amount of bitflips observed per round, and with $N_n \geq 0$. It is immediate that

$$\sum_{n=0}^{T} N_n = N_R.$$

Now, let us add an additional pair to this set, $(T+1, 0)$, in order to indicate that there are no rounds with more than T bitflips. Eq. (8) predicts the expected value of N_n, $N_r(n)$, which is written in terms of the unknown values μ_1 , μ_2, ..., μ_m. Therefore,

it seems reasonable to estimate these values as the ones that minimize the sum of the squared differences (SSD) between N_n and $N_r(n)$, defined as

$$SSD = \sum_{n=0}^{T+1} (N_n - N_r(n))^2. \tag{11}$$

It is worth mentioning that this is not the only possible figure-of-merit that one could use for the fitting, but it is widely accepted in science despite the fact that it is quite sensitive to outlier values. The following step is to find the best-fit values for the unknown parameters $\mu_1, \mu_2, \ldots, \mu_m$. In some cases like linear regression it is possible to get closed forms for the unknown parameters, but the complexity of Eq. (5) makes this strategy inadequate. Hence, in this case, this optimization problem was addressed by using two well-known techniques: Gradient-Descent (GD) [13] and Genetic Algorithms (GA) [14], which are implemented in the `Optim` [15] and `Evolutionary` [16] packages of the Julia language [17], [18]. With the estimated values for $\mu_1, \mu_2, \ldots \mu_m$, it is therefore possible to estimate the expected number of i-multiplicity MCUs, $N_{E,i}$, occurred in the whole experiment as

$$N^*_{E,i} = N_R \cdot \mu^*_i, \tag{12}$$

and the cross-section of every kind of event as

$$\sigma^*_i = N_R \cdot \mu^*_i / \Phi_T.$$

The asterisk is used as a superscript to distinguish the value estimated by this method from the actual one. For either of these two methods, an iterative approach is applied consisting in increasing the value of m in the range $[1, 8]$, since multiple events of larger size are not so frequent and strongly require longer computation times. Thus, for each possible value of m in this range, the GD or the GA method then yields as output the best possible fitting for $\mu_1, \mu_2, \ldots \mu_m$ among the ones found throughout the whole search space.

To optimize calculations, all the fittings that do not accomplish the well-known Pearson's χ^2-test with 95 % confidence and $\nu = (T + 2) - m$ degrees of freedom[2] must be rejected. This statistical parameter is defined as

$$\chi^2_M = \sum_{n=0}^{T+1} \frac{(N_n - N_r(n))^2}{N_r(n)}, \tag{13}$$

while the condition to be accomplished is that

$$\chi^2_{INV}(\nu, 0.95) < \chi^2_M < \chi^2_{INV}(\nu, 0.05), \tag{14}$$

$\chi^2_{INV}(\nu, 0.95)$ and $\chi^2_{INV}(\nu, 0.05)$ being the values of the inverse-χ^2 distribution with 95%-confidence ($0.05 = 1 - 0.95$). These two values define the bounds for realistic experiments. The higher is related to the deviation of the data from the proposed probability distribution due to random variations, the lower to excessive closeness to the expected values to be realistic, often due to overfitting. Any fitting with a χ^2_M not passing this test is irremediably dismissed. Finally, among the fittings that did pass the previous test, we chose the one that passes the modified Akaike Information Criterion [19] by minimizing

$$AIC = 2 \cdot m + 2 \cdot \ln(SSD_m) + \frac{2 \cdot m^2 + 2 \cdot m}{(T + 2) - m - 1}, \tag{15}$$

m being the maximum multiplicity for the fit and SSD_m its related sum of squared differences. The fraction included in the expression is added to deal with datasets with few values.

IV. Experimental Results

A. COTS 130-nm SRAM under neutrons

Firstly, the GD and GA methods were evaluated with experimental data obtained in a COTS bulk 130-nm SRAM presented by the authors in a previous work [6]. Three tests were carried out in that occasion, with N_R = 117, 120 and 119 rounds of reading each. These are described in Table I, which also shows the values of N_0, N_1, ..., N_{10} for each one of them.

Table II shows the predictions for $N^*_{E,i}$ issued by the GD and GA methods from (12). Two additional parameters are included for the sake of comparison:

- A Manhattan-Distance (MD)-based approach that consisted in grouping bitflips that were close to each other in the same MCU using a threshold distance as criteria. This made possible to know the number and multiplicity of MCUs that occurred in each round since the authors had access to the physical layout of the device. This method is the standard to exactly know the number and multiplicity of the events, $N_{E,i}$.
- The statistical method developed by the authors in previous works [6], [7], and briefly described in Section I.

[2]Number of dots to fit, $T + 2$, minus the number of parameters to fit, m.

TABLE I
TESTS CARRIED OUT UNDER A COTS SRAM [6], NOW USED IN THIS PAPER AS EXPERIMENTAL STUDY. N_n IS THE NUMBER OF ROUNDS WHERE n BITFLIPS WERE REGISTERED, N_R THE TOTAL NUMBER.

	Test 1	Test 2	Test 3		Test 1	Test 2	Test 3
N_0	59	48	55	N_6	1	0	2
N_1	30	35	36	N_7	0	1	3
N_2	11	17	14	N_8	–	1	0
N_3	7	11	5	N_9	–	0	–
N_4	9	6	3	N_{10}	–	–	–
N_5	0	1	1	N_R	117	120	119

TABLE II
NUMBER OF EVENTS WITH DIFFERENT MULTIPLICITIES, (i, $N^*_{E,i}$), ESTIMATED BY THE GD, GA AND MD-BASED METHODS, PLUS THE STATISTICAL ONE PRESENTED IN [6], [7]

	i	$N^*_{E,i}$ (GD)	$N^*_{E,i}$ (GA)	$N_{E,i}$ (MD-based)	Statist.
Test 1	1	58.8±15.3	57.9±15.2	62	65
	2	5.8±4.8	7.2±5.4	10	10
	3	8.1±5.7	9.4±6.1	5	6
	4	8.0±5.7	6.5±5.1	2	3
	5	–	–	2	–
Test 2	1	87.6±18.7	90.1±19.0	100	104
	2	10.3±6.4	9.3±6.1	13	13
	3	12.0±6.9	12.0±6.9	2	4
	4	–	–	2	1
	5	–	–	0	–
	6	–		1	–
Test 3	1	70.0±17.7	78.2±17.7	81	84
	2	4.5±4.3	5.2±4.6	13	12
	3	$\leq$ 5.4	$\leq$6.9	2	3
	4	$\leq$5.4	4.2 ± 4.1	4	3
	5	≈ 0	$\leq$1.2	–	–
	6	4.8 ± 4.4	≤ 5.6	–	–

In all cases, error margins were calculated as $2 \cdot \sqrt{N^*_{E,i}}$. Then, Fig. 2 shows the experimental values (N_n) and the estimated ones ($N_r(n)$) for the fittings yielded by the GA method for different values of m.

From Table II, one can observe that the GD and GA methods are less successful than the other known methods at predicting with accuracy the number of MCUs (multiplicity ≥ 2), especially in those cases with few occurrences. A possible reason could be that more rounds of reading are needed to obtain a greater accuracy. In fact, the χ^2-test (Eq. (14)) is known to be inaccurate if the input parameters (in this case, N_n and $N_r(n)$) are lower than 5 [20]. On the other hand, there is not enough evidence to state if there is one method more efficient than the other, although the GD method is faster and requires less computational resources.

B. Fitting to a Very Large Dataset

Both methods were also challenged with a larger dataset. In [21], Wilson *et al.* tested an Artix-7 XC7A200T-1SBG484C FPGA, with many identical rounds under neutrons. Fig. 4 of [21] showed the amount of rounds vs. number of bitflips per round, which is now recreated in Fig. 3. In [21], the authors postulated that the histogram was depicted by a simple Poisson distribution with $\mu \approx 6.0$; i.e., it was assumed that MCUs did not occur. However, Fig. 3 shows that this fit is not accurate (line $N_r(n)$ for $m = 1$), although this fact does not invalidate the rest of the study and conclusions of that paper. Table III shows the different fitting parameters as well as their SSD and AIC values. Thus, the occurrence of events with size up to 6–7 is very reallistic, which is in agreement with this family of FPGAs, where MCU are commonly observed [3], [22]. Finally, it is possible to determine by means of the expressions by Tausch [23] that the probability of misleading SBUs in close cells with MCUs is really small (0.2% if the number of bitflips is 20, 0.01% if it is 5).

C. Incomplete set of data

Finally, a variant of this method can be used to estimate the SBU/MCU rates in experiments where the number of rounds with no bitflips is unknown. In fact, it is possible that, during the execution of experiments only the information about rounds containing bitflips is stored, and rounds without them are discarded. Therefore, the actual value of N_R is unknown, so Eq. (8)

TABLE III
VALUES OF μ_i AND SSD FOR THE SIX FITS SHOWN IN FIG. 3

m	i	μ_i^*	i	μ_i^*	i	μ_i^*	SSD	AIC
1	1	5.408	–	–	–	–	$1.25{\cdot}10^{-2}$	417.2
2	1	1.575	2	1.995	–	–	$1.38{\cdot}10^{-3}$	322.8
3	1	2.219	2	0.452	3	0.865	$1.75{\cdot}10^{-4}$	234.7
4	1	2.263	2	0.802	3	0.219	$6.9{\cdot}10^{-5}$	196.9
	4	0.319	–	–	–	–		
5	1	2.173	2	0.874	3	0.387	$4.6{\cdot}10^{-5}$	181.9
	4	0.0	5	0.151	–	–		
6	1	2.188	2	0.829	3	0.451	$3.9{\cdot}10^{-5}$	179.1
	4	0.039	5	0.0042	6	0.082		
7	1	2.186	2	0.838	3	0.421	$3.1{\cdot}10^{-5}$	173.1
	4	0.085	5	0.013	6	0.000		
	7	0.050	–	–	–	–		

cannot be applied to determine $N_r(n)$. The solution is just to renormalize $P_G(n)$, given by Eq. (5), to take into account that experimental data for $n = 0$ are not available. From Eq. (6) it is possible to deduce that

$$N_r(n) \approx N_R^+ \cdot \frac{P_G(n)}{1 - P_G(0)} = \\ = N_R^+ \cdot \frac{P_G(n)}{1 - \exp\left(-\sum_{i=1}^{m} \mu_i\right)}, \tag{16}$$

N_R^+ being the number of rounds with observed bitflips. With this value of $N_r(n)$, and as explained before, Eq. (11) must be applied to obtain the best fitting to μ_1, μ_2, ..., μ_n. In this case, the first element of the sum inside Eq. (11) must be $n = 1$ instead of $n = 0$, as there is no information about this value. As in this situation there are only $T + 1$ points to fit, the value of ν, the number of freedom degrees used in Eqs. (13)-(14) turns $T + 1 - (m + 1) = T - m$.

This variant has been used with another dataset obtained in 2011, with a platform with 64 90-nm CMOS SRAMs (2 GBit) and validated at CERF-EU [24]. As the system did not record the cycles where no events were detected, the results are appropriate to investigate if the variant proposed in this section works under these conditions.

During this test, there were 182 rounds where 292 bitflips were registered and categorized in events of different multiplicity using other statistical techniques implemented in the LELAPE tool [25], [26] and shown on Table IV. The histogram in Fig. 4 classifies the rounds according to the number of observed bitflips in each one of them. Besides, the different fittings minimizing AIC with either gradient descent (GD) or genetic algorithms (GA) are displayed in the figure as well.

TABLE IV
EVENT CATEGORIZATION OF THE EXPERIMENT CARRIED OUT IN CERF-EU IN 2011 WITH 90-NM COTS SRAMS (292 BITFLIPS IN 182 ROUNDS OF READING)

Multiplicity (i)	LELAPE	$N_{E,i}^*$ (GD)	$N_{E,i}^*$ (GA)
1	155	250.4	246.8
2	36	0.0	0.13
3	11	0.0	2.8
4	4	9.4	8.4
N_T	292	288.0*	288.1*

This strategy was tested with the data shown in Table I & Fig. 2 after removing N_0, or number of empty rounds. In general, the results are quite similar to those shown in Table II although the lesser information leads to make some big mistakes (e.g., the number of estimated SBUs for Test 1 was 32.2 for the GD method, far from the more accurate 57.9 & 58.8 shown in Table II).

In spite of the fact of having found parameters that seem to accurately fit the values in the histogram, the number of estimated events is quite far from the actual values got using the Manhattan-distance method. Provided that the number of rounds without bitflips is not negligible and that it is a key data input to calculate the fitting, any error in the estimation is enlarged and transmitted to the final results. We consider that the number of cycles without bitflips is on the order of rounds with bitflips, so accurate calculations are quite difficult to do. This strategy should be used only when no other alternative is feasible (e.g., checking old datasets where only rounds with bitflips were recorded).

TABLE V
VALUES OF TABLE II IF N_0 HAD NOT BEEN RECORDED.

	i	$N^*_{E,i}$ (GD)	$N^*_{E,i}$ (GA)	$N_{E,i}$ (MD-based)	Statis.
Test 1	1	32.2±11.3	71.7±16.9	62	65
	2	11.3±6.7	≤2.1	10	10
	3	7.2±5.4	14.6±7.6	5	6
	4	9.4±6.1	–	2	3
	5	–	–	2	–
Test 2	1	87.4±18.7	76.6±17.8	100	104
	2	10.4±6.4	16.3±8.1	13	13
	3	12.0±6.9	10.9±6.6	2	4
	4	–	–	2	1
	5	–	–	0	–
	6	–		1	–
Test 3	1	85.4±18.5	77.9±17.7	81	84
	2	≈0	5.1±4.5	13	12
	3	≤ 7.1	≤6.3	2	3
	4	≤4.5	≤0.7	4	3
	5	≈ 0	≤4.5	–	–
	6	5.0±4.5	≤7.7	–	–

V. PROPOSAL OF GUIDELINES TO VALIDATE RADIATION TESTS

The strategy of fitting the histogram with information about the number of bitflips per round has shown to be a new option to categorize the events according to their multiplicity and to estimate the SBU/MCU event rates. However, even though we can consider that this technique can be further explored in the future, it is not mature enough to oust other statistical techniques [1], [3]–[7], which have shown more accurate estimations and are not restricted to a special case of radiation test. Another observed issue is that the fitting processes, especially those based on genetic algorithms, can take several minutes until reaching the optimal value. Therefore, it is nonsense to try to look for hypothetical very large events.

Nevertheless, the theoretical study have other possible applications. For example, it is very useful to decide time between consecutive scrub cycles to remove accumulated errors, as it was demonstrated in [27]. Even more, it provides appropriate criteria to determine if radiation experiments are correctly done and issued data interpreted. In contrast, the other techniques only provide tools to estimate false multiple events [23], [28]–[30]. These points will be studied in the following sections.

A. Radiation tests with very low flux

This situation corresponds to experiments on memories the internal structure of which is unknown exposed to such a low flux that one can assume than only one or zero events occur per cycle, so the number of bitflips observed in every reading round is just the multiplicity of the unique event that occurred. This strategy has been proposed by some authors [31], [32] to determine the cross section for multiple events of different multiplicity.

Using the same nomenclature as Section III, let us suppose that we perform a radiation experiment with N_R rounds in which we detect N_n rounds with n bitflips, $n \in 0, 1, \ldots, T$. If we assume that only zero or one event occurred per round, and that N_n is just the number of n-size MCUs, the experimental expected number of n-size events per round is

$$\mu^*_n = \frac{N_n}{N_R}. \tag{17}$$

This assumption only holds if the probability of an event of n-size is much larger that the sum of all the possible combinations of events of smaller multiplicities that produce that number of bitflips. For example, the probability of that of observing a 2-bit MCU must be much higher than observing 2 SBUs, or that of observing a 3-bit MCU much larger than the sum of the probabilities of observing in one round thre SBUs, or one 2-bit MCU with one SBU, etc. From Eq. (5), these conditions eventually yield the following inequalities:

$$\mu^*_2 \gg \frac{1}{2} \cdot \mu^{*2}_1,$$
$$\mu^*_3 \gg \frac{1}{6} \cdot \mu^{*3}_1 + \mu^*_1 \cdot \mu^*_2,$$

and

$$\mu^*_4 \gg \frac{1}{24} \cdot \mu^{*4}_1 + \mu^*_1 \cdot \mu^*_3 + \frac{1}{2} \cdot \mu^{*2}_1 \cdot \mu^*_2 + \frac{1}{2} \cdot \mu^{*2}_2.$$

Other expressions for larger values of n can be determined, but they are not presented given their growing complexity. If these inequalities are not hold by the experimental values, the analysis is inconsistent and another method to separate events must be used instead.

B. Variation of the physical parameters during radiation experiments

The mathematical model developed in Section II must work on any radiation test not only with a sufficiently high number of reading rounds, but also with stable rates of events per round (hence, constant round duration, cross sections and radiation flux, or, at least, the product of the three parameters). Only the condition of stable radiation flux can be relaxed if the mean fluence value per round is constant. This allows applying the model to radiation sources such as linear proton or neutron beams, in which the radiation is done with trains of periodical short but intense pulse. If the time between pulses is much lower than the round duration, we can consider that the mean radiation flux is almost constant just using the well known Nyquist's theorem.

Let us give an illustrating example: there is a large set of memories used to know the soft error rate (SER) associated with radioactive impurities, such as the experiment that is depicted in [33]. Alpha particles can induce single event upsets (SEU) of different multiplicity, which should be easily detectable using statistical techniques or layout if available. In general, the radiation flux is constant if the impurities are in secular equilibrium [34], but if during the source manufacturing process this equilibrium is broken, the radiation flux changes in time. In the aforementioned paper, Gedion *et al.* predicted that, in some circumstances, the emission of alpha particles can grow 4 times in only one year.

Fig. 5 shows the Monte Carlo simulations of two experiment to detect the alpha soft error rate. In the first one, labeled as *S. Eq.* in the figure, it was supposed that expected number of events per round was constant and set to $\mu_1 = 1$, $\mu_2 = 0.2$ and $\mu_3 = 0.04$. This stability disappears in the second test, labeled as *N. Eq.* in the figure, where it was supposed that the SERs linearly shift in time, the final values being four times the initial ones, but the average values were identical to those of the first simulation. In both cases, $N_R = 1000$ rounds were simulated, and the program recorded the total number of SBUs and MCUs, from which the experimental values of μ_i^* were calculated as if we were doing an actual radiation test.

Bars in the graph show the number of rounds with different number of bitflips. Dash and dash-dot lines indicate the expected values deduced from Eqs. (5) and (8) using the observed values of μ_1^*, μ_2^* and μ_3^*. In the case of secular equilibrium, bars and the dashed line are quite close to each other. This does not occur in the case of the simulations in non equilibrium, showing an excess of rounds with no bitflips. These facts affect the p-value to evaluate the goodness of fit. This parameter is defined from the value of χ^2_M for this set of data, defined in Eq. 13, as

$$p = 1 - \chi^2_{CMF}\left(\chi^2_M, \nu\right), \tag{18}$$

χ^2_{CMF} being the CMF for the χ^2-distribution and ν the degrees of freedom. This statistical parameter is widely used in many fields of science to decide if the hypothesis is compatible with experimental data. Thus, if $p < 0.05$, the hypothesis of the histogram fitting the expected distribution, (Eq. (5)), must be discarded. In the examples shown in Fig. 5, data simulated in secular equilibrium pass this test, whereas data in nonsecular equilibrium do not. However, given the probabilistic nature of the p-value test, it was observed running several simulations that sometimes data sets issued from constant SERs were rejected, whereas data sets from changing rates did pass the test.

Another way of testing the hypothesis of stable SER consists in investigating the number of rounds without bitflips between rounds with them. It is easy to deduce that the probability of observing bitflips in the round q and not doing that again until round $q + d$ is

$$P_{DIS}(d) = P_G(0)^{d-1} \cdot (1 - P_G(0)), \tag{19}$$

$P_G(0)$ being Eq. (6) using the measured values of μ_i^* as arguments. Unlike Eq. (5), this probability distribution is just the geometric distribution, easy to calculate and deeply studied. Fig. 6 shows the histogram for the values of d derived from the same simulation as in Fig. 5. As expected, the simulation in secular equilibrium follows the theoretical calculation, while that with increasing rates does not. This can be evaluated using the p-value, defined as in Eq. (18), which demonstrates that the bars in the figure are not compatible with an experiment with stable SERs.

Apparently, this distance test seems to be more powerful and accurate than that based on checking the bitflips in rounds, correctly rejecting what had been erroneously accepted by the latter.

This allows using another approach. If the experimental values of μ_i^* are known, other partial tests can be done. Hence, restraining to events with i-multiplicity, one can extract those rounds in which they where registered, determine the number of rounds with k events of this sort, or just looking for the d parameter between rounds with detections. If the SER for this parameter is constant, the experimental probability distributions should look like Poisson distributions or derived from it, such as that of Eqs. (2) or (19). Table VI shows the results of performing 10000 times the simulations of Figs. 5 and 6 and determining the percentage of successful identifications for the distribution of bitflips-per-round and distance between rounds with events using the global probability distribution and the simple Poisson distibution for events of different sizes. According to the results shown in this table, the most successful tests are those bases on distances for global distribution and for SBUs, the rest of tests sometimes unable to detect variations in the SER.

Finally, it is worth listing situations in which this test can be applied. In spite of the fact that the example chosen to illustrate this method is that of a set of memories where the radioactive impurities change their emissivity in time, it is feasible to apply it in any tests where the expected SER is not stable. Some possible situations could be the following:

- In proton, neutron or radiation campaigns, the SERs per round will change if the flux shifts, if the beam section shrinks or broadens or the beam axis stops being correctly aligned, or if the applied power supply value fluctuates.

TABLE VI
PERCENTAGE OF CORRECT IDENTIFICATIONS OF TESTS WITH AND WITHOUT SECULAR EQUILIBRIUM ACCORDING TO THE TEST OF DIFFERENT STATISTICAL PARAMETERS.

	Multiplicity, i	Test	Sec. Eq.	N. Sec. Eq.
Global		Bitflips in rounds	84.9 %	68.9 %
		Distance	85.7 %	97.6 %
Partial	1	Bitflips in rounds	92.1 %	54.6 %
		Distance	89.5 %	92.3 %
	2	Bitflips in rounds	93.3 %	11.8 %
		Distance	79.1 %	73.2 %
	3	Bitflips in rounds	97.7 %	3.2 %
		Distance	61.9 %	67.5 %

- In radiation tests, to prove the synergistic effects between the accumulated total ionizing dose and the SEU cross sections. Typically, the combination of these effects is investigated using a preliminary irradiation with gamma rays followed by heavy ions [35]–[38]. In all these works a significant change in the cross section was observed, which could be also detected with the procedure shown in this section in radiation-ground tests that just focus on provoking events on the DUT, not dose accumulation (i.e., ^{60}Co tests).
- In real time tests, to detect variations in the radiation flux due to changes in the surrounding environment (presence of water in air or ice on roofs), solar activity, accidental placement of bulky elements nearby, etc.

C. Detection of forged experimental data

Section II establishes the properties that experimental data have to accomplish. Therefore, results that do not pass the χ^2 test (Eq. (14)) should be put in quarantine as suspicious of erroneous treatment or, in worst case, forgery.

Let us suppose that someone performs a radiation test on a memory or FPGA and just collects a huge set of small size events. Then, they decide to manually introduce events of larger size to make the results more interesting. Fig. 7 depicts the following scenario. The experiment only cast SBU and 2-bit MCUS, so the researcher decides to roguely add a few fake 3-bit and 4-bit events to those cycles where only one SBU occurred. But this action slightly changes the shape of the histogram, changing the value of the χ^2_M, dramatically reducing the p-value and allowing the detection of the fraud.

VI. CONCLUSIONS

This paper has presented a model to depict the statistical characteristics found in radiation experiments with many reading rounds. This allows proposing two methods to estimate the SBU/MCU rates in radiation-ground tests on memory devices consisting in a large amount of rounds of reading performed under identical conditions. These methods perform a best-fit approach using Gradient Descent (GD) or a Genetic Algorithm (GA) to look for solutions in the entire search space. They have proved to be accurate in estimating SBU/MCU rates in experimental results carried out by the authors in previous works on COTS SRAMs [6] and FPGAs [21]. Besides, it is demonstrated that it is possible to determine if the characteristics of the tests have not changed along the experiments and to propose tests that, if not passed, can point out to the possibility of the data having been altered.

Finally, it is worth highlighting that all the software used in this study do not need any proprietary information of the manufacturer of the device under test and they are quite easy to implement in common programming languages. For example, the code used in this work is available on https://zenodo.org/records/14810983.

REFERENCES

[1] X. Wang *et al.*, "A Statistical Method for MCU Extraction Without the Physical-to-Logical Address Mapping," *IEEE Trans. Nucl. Sci.*, vol. 67, no. 7, pp. 1443–1451, Jul. 2020. doi: 10.1109/TNS.2020.2982033.
[2] J. Guo *et al.*, "The Bitmap Decryption Model on Interleaved SRAM Using Multiple-Bit Upset Analysis," *IEEE Trans. Nucl. Sci.*, vol. 69, no. 8, pp. 1857–1864, Aug. 2022. doi: 110.1109/TNS.2022.318608.
[3] M. Wirthlin, D. Lee, G. Swift, and H. Quinn, "A Method and Case Study on Identifying Physically Adjacent Multiple-Cell Upsets Using 28-nm, Interleaved and SECDED-Protected Arrays," *IEEE Trans. Nucl. Sci.*, vol. 61, no. 6, pp. 3080–3087, Dec. 2014. doi: 10.1109/TNS.2014.2366913.
[4] A. Pérez-Celis and M. J. Wirthlin, "Statistical Method to Extract Radiation-Induced Multiple-Cell Upsets in SRAM-Based FPGAs," *IEEE Trans. Nucl. Sci.*, vol. 67, no. 1, pp. 50–56, Jan. 2020. doi: 10.1109/TNS.2019.2955006.
[5] S. Gao *et al.*, "Heavy ion-induced MCUs in 28-nm SRAM-based FPGAs: upset proportions, classifications, and pattern shapes," *Nuclear Science and Techniques*, vol. 33, no. 12, p. 161, Dec. 2022. doi: 10.1007/s41365-022-01142-7.
[6] J. A. Clemente *et al.*, "Statistical Anomalies of Bitflips in SRAMs to Discriminate SBUs From MCUs," *IEEE Trans. Nucl. Sci.*, vol. 63, no. 4, pp. 2087–2094, Aug. 2016. doi: 10.1109/TNS.2016.2551263.
[7] F. J. Franco *et al.*, "Statistical Deviations From the Theoretical Only-SBU Model to Estimate MCU Rates in SRAMs," *IEEE Trans. Nucl. Sci.*, vol. 64, no. 8, pp. 2152–2160, Aug. 2017. doi: 10.1109/TNS.2017.2726938.
[8] J. C. Fabero *et al.*, "Single Event Upsets Under 14-MeV Neutrons in a 28-nm SRAM-Based FPGA in Static Mode," *IEEE Trans. Nucl. Sci.*, vol. 67, no. 7, pp. 1461–1469, Jul. 2020. doi: 10.1109/TNS.2020.2977874.

[9] V. Vlagkoulis *et al.*, "Single Event Effects Characterization of the Programmable Logic of Xilinx Zynq-7000 FPGA Using Very/Ultra High-Energy Heavy Ions," *IEEE Trans. Nucl. Sci.*, vol. 68, no. 1, pp. 36–45, Jan. 2021. doi: 10.1109/TNS.2020.3033188.

[10] A. Pérez-Celis, C. Thurlow, and M. Wirthlin, "Identifying Radiation-Induced Micro-SEFIs in SRAM FPGAs," *IEEE Trans. Nucl. Sci.*, vol. 68, no. 10, pp. 2480–2487, Oct. 2021. doi: 10.1109/TNS.2021.3108572.

[11] P. Reviriego and J. A. Maestro, "A technique to calculate the MBU distribution of a memory under radiation suffering the event accumulation problem," in *2008 European Conference on Radiation and Its Effects on Components and Systems*, pp. 393–396, Sept. 2008. doi: 10.1109/RADECS.2008.5782750.

[12] C. M. Grinstead and J. L. Snell, *Introduction to Probability*. American Mathematical Society, 2nd ed., 2003. [Online]. Available on https://math.dartmouth.edu/∼prob/prob/prob.pdf.

[13] S. Boyd and L. Vandenberghe, *Convex Optimization*, ch. 9.3, pp. 463–466. Cambridge University Press, 7th ed., 2009. ISBN: 978-0-521-83378-3.

[14] K. Tang, K. Man, S. Kwong, and Q. He, "Genetic algorithms and their applications," *IEEE Signal Process. Mag.*, vol. 13, no. 6, pp. 22–37, Nov. 1996. doi: 10.1109/79.543973.

[15] P. K. Mogensen and A. N. Riseth, "Optim: A mathematical optimization package for Julia," *Journal of Open Source Software*, vol. 3, no. 24, no. 24, 2018. Art. 615. doi: 10.21105/joss.00615. The tool is available on https://julianlsolvers.github.io/Optim.jl/stable/.

[16] A. Wilde *et al.*, "Evolutionary.jl," July 2021. doi: 10.5281/zenodo.5110647. [Online]. Available on https://wildart.github.io/Evolutionary.jl/dev/.

[17] "The Julia Programming Language," 2024. [Online]. Available on https://julialang.org/.

[18] J. Bezanson, A. Edelman, S. Karpinski, and V. B. Shah, "Julia: A fresh approach to numerical computing," *SIAM Review*, vol. 59, no. 1, no. 1, pp. 65–98, 2017. doi: 10.1137/141000671.

[19] H. Akaike, "A new look at the statistical model identification," *IEEE Trans. Autom. Control*, vol. 19, no. 6, pp. 716–723, Dec. 1974. doi: 10.1109/TAC.1974.1100705.

[20] R. E. Walpole, R. H. Myers, S. L. Myers, and K. Ye, *Probability & Statistics for Engineers & Scientists*. 9th ed., 2012.

[21] A. E. Wilson *et al.*, "Neutron Radiation Testing of a TMR VexRiscv Soft Processor on SRAM-Based FPGAs," *IEEE Trans. Nucl. Sci.*, vol. 68, no. 5, pp. 1054–1060, May 2021. doi: 10.1109/TNS.2021.3068835.

[22] B. Du *et al.*, "Ultrahigh Energy Heavy Ion Test Beam on Xilinx Kintex-7 SRAM-Based FPGA," *IEEE Trans. Nucl. Sci.*, vol. 66, no. 7, pp. 1813–1819, July 2019. doi: 10.1109/TNS.2019.2915207.

[23] H. J. Tausch, "Simplified Birthday Statistics and Hamming EDAC," *IEEE Trans. Nucl. Sci.*, vol. 56, no. 2, pp. 474–478, Apr. 2009. doi: 10.1109/TNS.2009.2012710.

[24] M. Silari and F. Pozzi, "The CERN-EU high-energy Reference Field (CERF) facility: applications and latest developments," *EPJ Web Conf.*, vol. 153, 2017. Art. no. 03001. doi: 10.1051/epjconf/201715303001.

[25] J. A. Clemente, M. Rezaei, J. C. Fabero, H. Mecha, and F. J. Franco, "LELAPE: An Open-Source Tool to Classify SEUs according to their Multiplicity in Radiation-Ground Tests on Memories," *IEEE Trans. Nucl. Sci.*, vol. 71, no. 10, pp. 2260–2671, Oct. 2024. doi: 10.1109/TNS.2024.3450607.

[26] F. J. Franco, J. A. Clemente, M. Rezaei, J. C. Fabero, and H. Mecha, "LELAPE," Dec. 2023. [Online]. Available for free use on https://doi.org/10.5281/zenodo.10156119.

[27] R. Ramezani, J. A. Clemente, and F. J. Franco, "Analytical reliability estimation of SRAM-based FPGA designs against single-bit and multiple-cell upsets," *Reliab. Eng. & Syst. Saf.*, vol. 202, 2020. Art. no. 107036. doi: 10.1016/j.ress.2020.107036.

[28] H. J. Tausch and H. Puchner, "Analysis of Hamming EDAC SRAMs Using Simplified Birthday Statistics," *IEEE Trans. Nucl. Sci.*, vol. 62, no. 4, pp. 1771–1778, Aug. 2015. doi: 10.1109/TNS.2015.2444272.

[29] F. J. Franco, J. A. Clemente, H. Mecha, and R. Velazco, "Influence of Randomness During the Interpretation of Results From Single-Event Experiments on SRAMs," *IEEE Trans. Device Mater. Reliab.*, vol. 19, no. 1, pp. 104–111, Mar. 2019. doi: 10.1109/TDMR.2018.2886358.

[30] F. J. Franco *et al.*, "Inherent Uncertainty in the Determination of Multiple Event Cross Sections in Radiation Tests," *IEEE Trans. Nucl. Sci.*, vol. 67, no. 7, pp. 1547–1554, Jul. 2020. doi: 10.1109/10.1109/TNS.2020.2977698.

[31] A. Manuzzato, S. Gerardin, A. Paccagnella, L. Sterpone, and M. Violante, "On the Static Cross Section of SRAM-Based FPGAs," in *2008 IEEE Radiation Effects Data Workshop*, pp. 94–97, July 2008. doi: 10.1109/REDW.2008.24.

[32] J. M. Bird *et al.*, "Neutron Induced Single Event Upset (SEU) Testing of Commercial Memory Devices with Embedded Error Correction Codes (ECC)," in *2017 IEEE Radiation Effects Data Workshop (REDW)*, pp. 119–126, Jul. 2017. doi: 10.1109/NSREC.2017.8115445.

[33] S. Martinie *et al.*, "Underground experiment and modeling of alpha emitters induced soft-error rate in CMOS 65 nm SRAM," *IEEE Trans. Nucl. Sci.*, vol. 59, no. 4, pp. 1048–1053, Aug. 2012. doi: 10.1109/TNS.2012.2189246.

[34] M. Gedion *et al.*, "Effect of the Uranium Decay Chain Disequilibrium on Alpha Disintegration Rate," *IEEE Trans. Nucl. Sci..*, vol. 58, no. 6, pp. 2793–2797, Dec. 2011. doi: 10.1109/TNS.2011.2172954.

[35] R. Koga, P. Yu, K. Crawford, J. George, and M. Zakrzewski, "Synergistic Effects of Total Ionizing Dose on SEU Sensitive SRAMs," in *2009 IEEE Radiation Effects Data Workshop*, pp. 127–132, July 2009. doi: 10.1109/REDW.2009.5336303.

[36] Q. Zheng *et al.*, "The Increased Single-Event Upset Sensitivity of 65-nm DICE SRAM Induced by Total Ionizing Dose," *IEEE Trans. Nucl. Sci.*, vol. 65, no. 8, pp. 1920–1927, Aug. 2018. doi: 10.1109/TNS.2018.2816583.

[37] Q. Zheng *et al.*, "Total Ionizing Dose Influence on the Single-Event Multiple-Cell Upsets in 65-nm 6-T SRAM," *IEEE Trans. Nucl. Sci.*, vol. 66, no. 6, pp. 892–898, June 2019. doi: 10.1109/TNS.2018.2875451.

[38] J. Cui, Q. Zheng, Y. Li, and Q. Guo, "Impact of High TID Irradiation on Stability of 65 nm SRAM Cells," *IEEE Trans. Nucl. Sci.*, vol. 69, no. 5, pp. 1044–1050, May 2022. doi: 10.1109/TNS.2022.3164654.

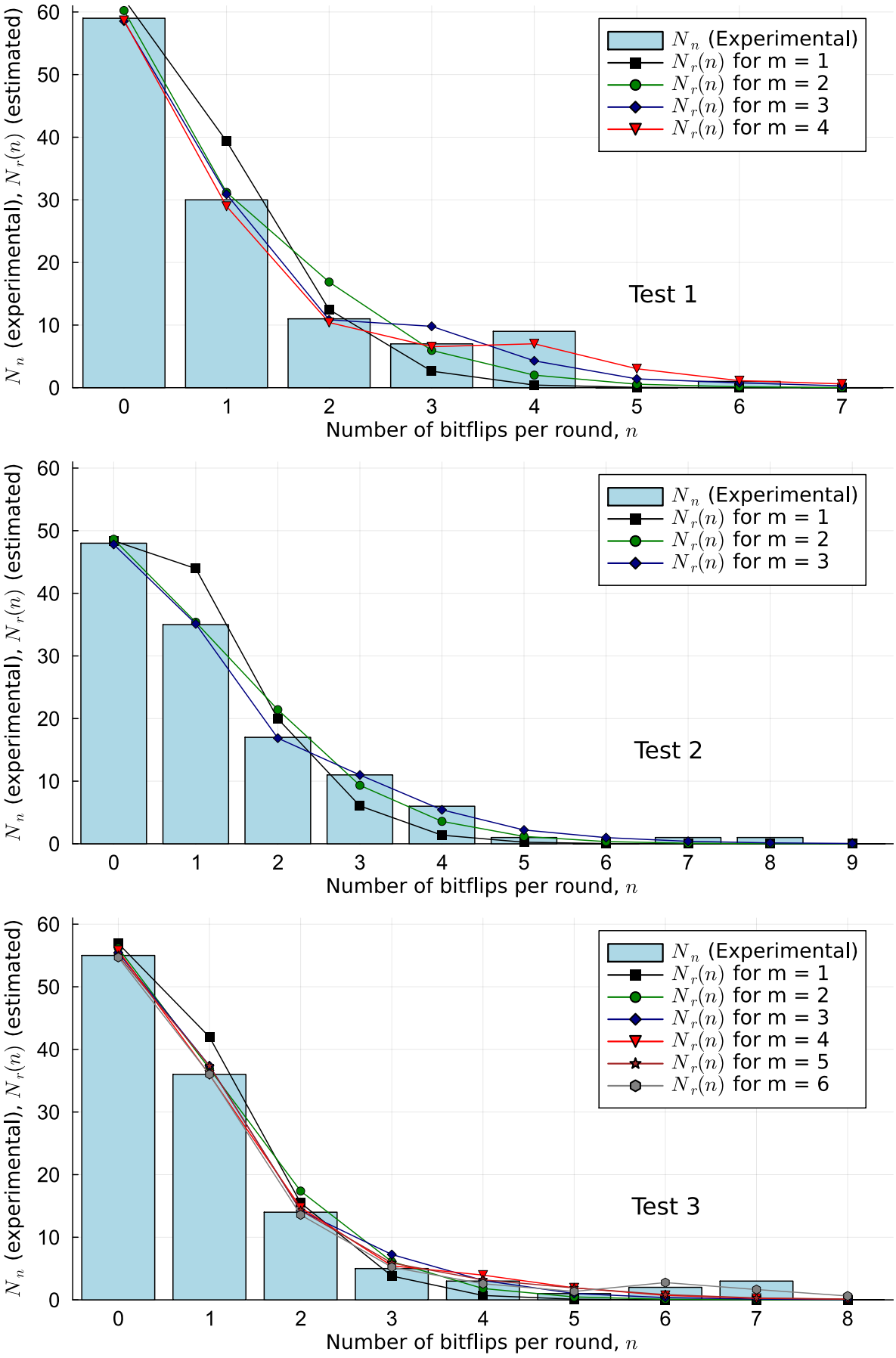

Fig. 2. N_n (from Test 1 in Table I) vs. $N_r(n)$ (from Eq. (8)) estimated by the GA approach, for different values of m. These were obtained with Eq. (8) using the values $\mu_1^*, \mu_2^*, \ldots \mu_m^*$ returned by the GA approach.

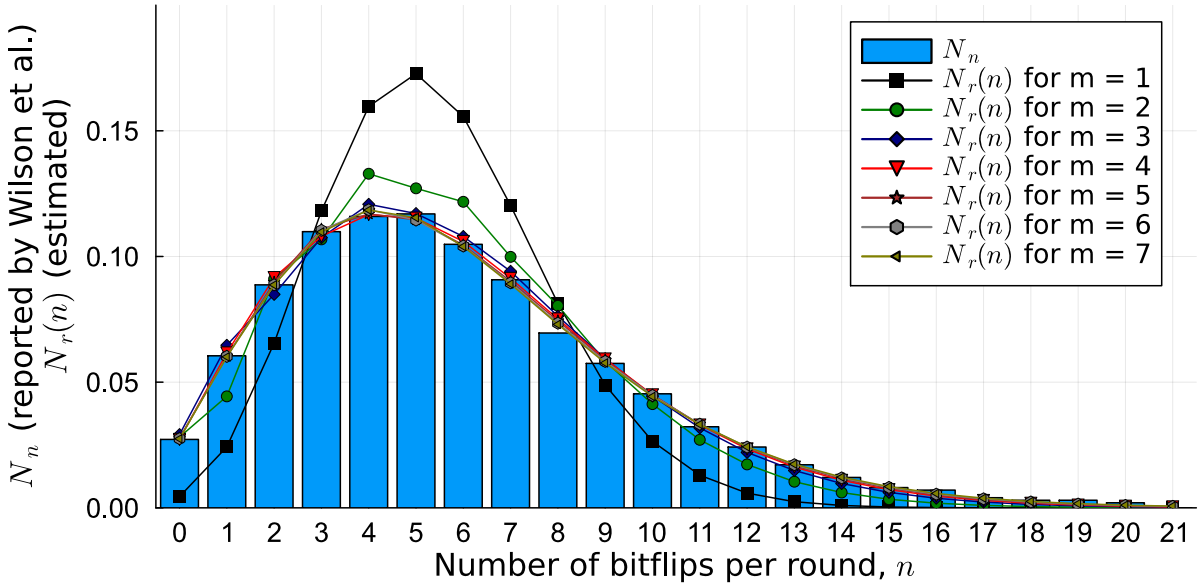

Fig. 3. N_n as reported in Fig. 4 of [21] (data sampled with Engauge Digitizer) vs. $N_r(n)$ predicted by the GD approach, for different values of m. N_n and $N_r(n)$ have been normalized to the total number of rounds of each experiment.

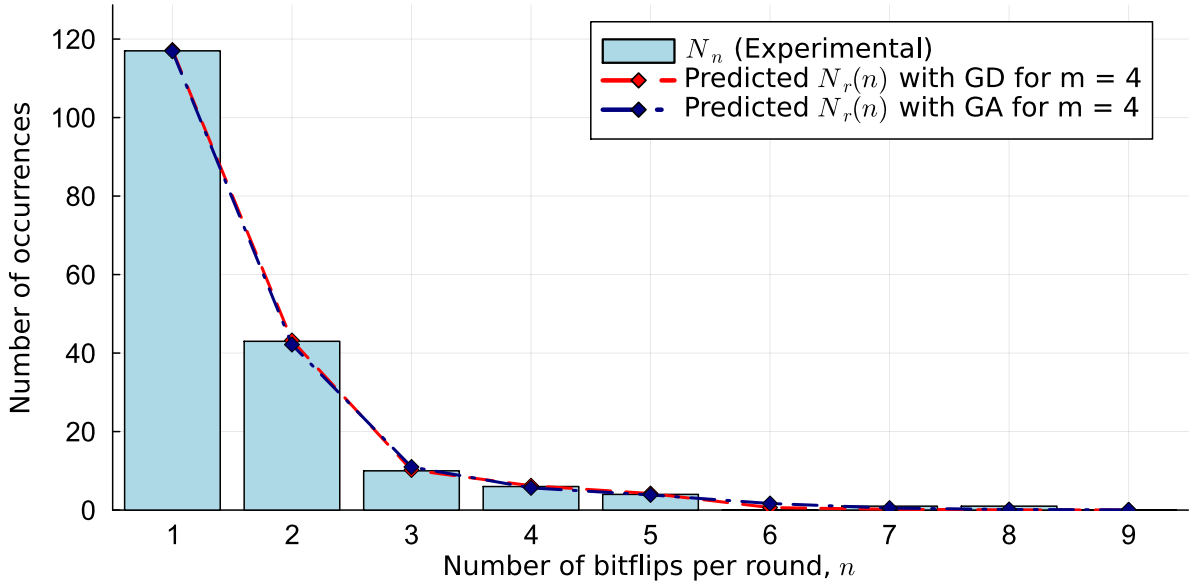

Fig. 4. Histogram obtained in experiments in CERF.

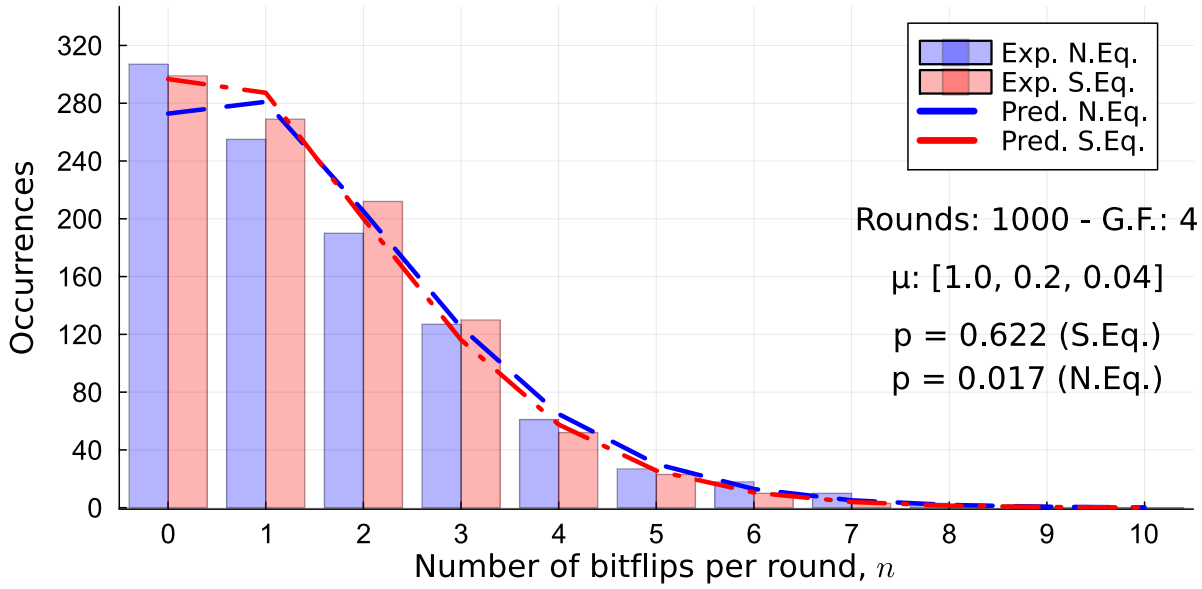

Fig. 5. Alpha-emission experiment. S. Eq: secular equilibrium; N. Eq: Non equilibrium. In both cases, Monte Carlo results (Exp.) and theoretical predictions. These were obtained using the experimental values of μ_i^*. The gain factor (G.F) indicates that the ratio betwen initial and final activity in non equilibrium was 4.

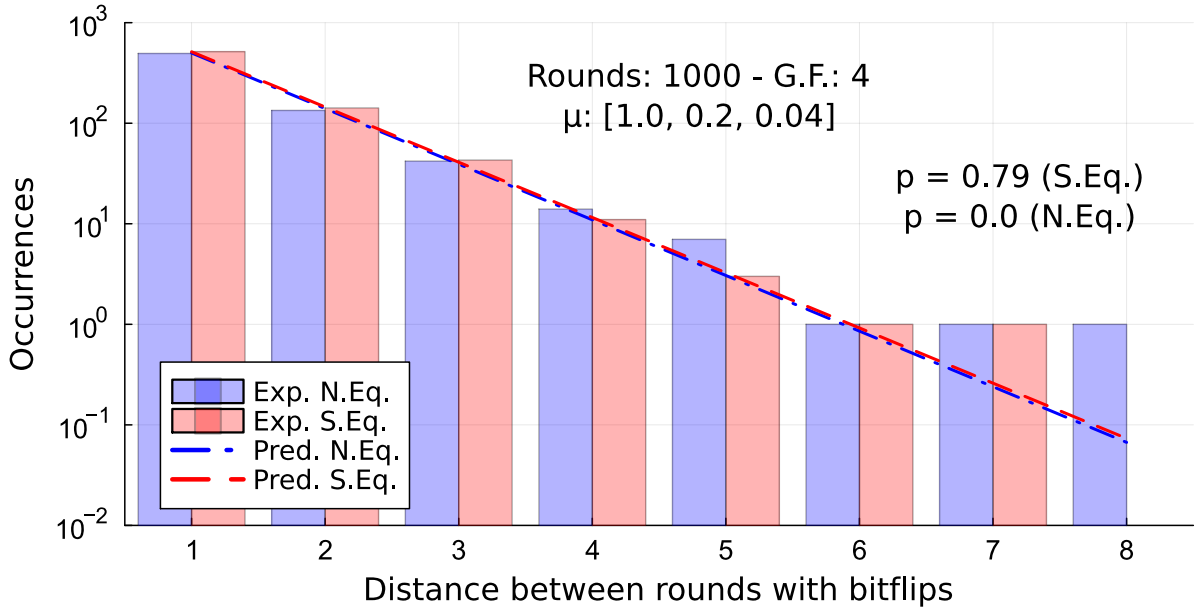

Fig. 6. Distance between consecutive rounds with bitflips. This graph derives from the same simulation as Fig. 5 does. The gain factor (G.F) indicates that the ratio betwen initial and final activity in non equilibrium was 4.

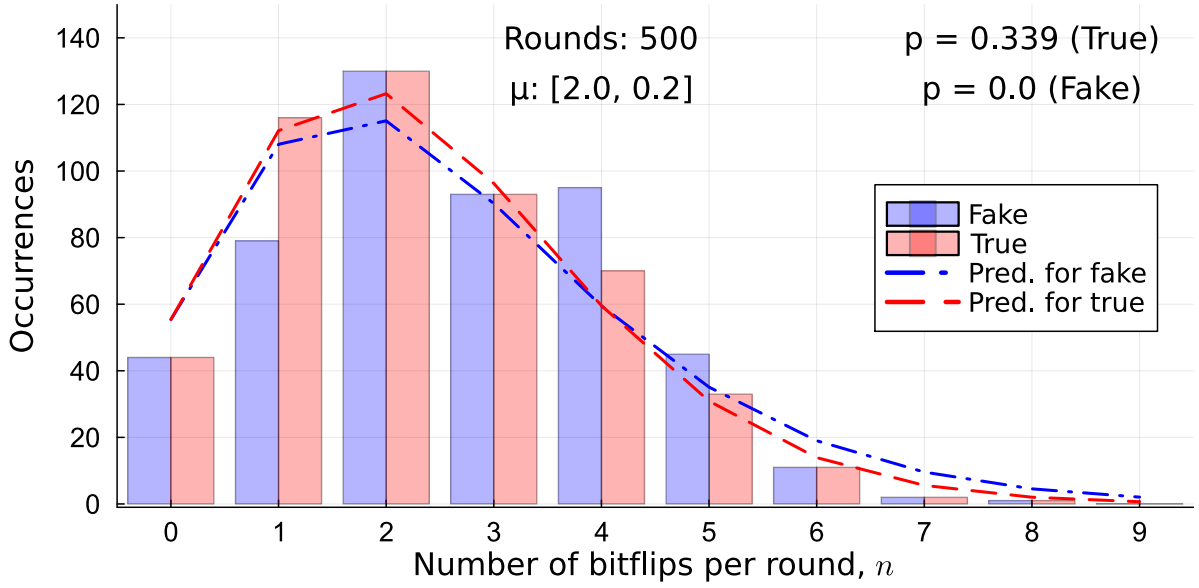

Fig. 7. Original vs. modified data set. The experiment detected 968 SBU and 114 2-bit MCU. 25 false 3-bit and 12 4-bit MCUs were added to the set of data, distorting the histogram shape.